Numerical and Physical Modeling of the Effect of Roughness Height on Cavitation Index in Chute Spillways

Abstract

This Study presents the results of physical and numerical modeling of the effect of bed roughness height of chute spillways on the cavitation index. A 1:50-scale physical hydraulic model of the chute spillway of Surk Dam was constructed at the hydraulic laboratory of Shahrekord University, Iran. The experiments were conducted for different flow rates and the parameters of pressure, velocity, and flow depth in 26 positions along the chute. Finally, the ANSYS-FLUENT model was calibrated in the chute spillway using the experimental data by assumptions of two-phase Volume of Fluid (VOF) and k–ε (RNG) turbulence models. The cavitation index in different sections of the chute spillway was calculated for different values of bed roughness including the roughness heights of 1, 2, and 2.5 mm. Results showed that the minimum values of the cavitation index were 0.2906, 0.2733, and 0.2471 for the roughness heights of 1, 2 and 2.5 mm, respectively. The statistical significance analysis showed that reducing the roughness height from 2.5 to 1 mm would not change significantly the value of the cavitation index at 95% confidence interval.

Keywords: Physical model, Spillway, Cavitation, ANSYS-FLUENT Software

Introduction

Chutes and ogee spillways are taken into account as the most important structures used in dam construction. These types of structures are at the risk of cavitation due to the high level and velocity of water flow [1]. Cavitation is the formation of vapor cavities in a liquid, which occurs at high-velocity flow, where the water pressure is reduced locally because of irregularities in the flow surface. As the vapor cavities move into a zone of higher pressure, they collapse, producing high-pressure shock waves. If the cavities collapse near a flow boundary, there will be damage to the material at the boundary [2]. Cracks, ramp offsets and surface roughness can increase the potential for cavitation damage. Many high-height Dam spillways are at the risk of damage due to the occurrence of the cavitation phenomenon. Three factors that contribute to the damage on spillway are flow velocity; material strength; and operating time [3]. Inozemtsev (1969) [4] studied the possibility of the occurrence of cavitation, particularly in high-velocity flows at the first part of spillway downstream, which can contribute to severe damages or structural failure. Kells and Smith (1991) [5] proposed a method for preventing or reducing cavitation damage on spillways using spillway aerators and they presented design considerations and criteria for the spillway aerators using physical hydraulic models. Studies also revealed that air entrainment increases with increase in Froude number, ramp height and cavity pressure.

Rajasekhar et al. (2014) [6] investigated the impact of existing voids on the spillway surface and proposed strategies to improve the cavitation resilience of the Sagar Dam spillway (India), the groovheight of 124.66m, located in the Krishna River using a numerical modelling approach. Tests were carried out at different flow rates on a 1:80 scale model and results revealed that in addition to the design flow rate, negative pressure exists even at flow rates below it. Based on the negative pressure measurement and cavitation index computation, the study concluded that cavitation leads to the corrosion of spillway surface and proposed aeration and creation of transverse grooves like the best and economic solutions to overcome this phenomenon. A 1:24-scale physical hydraulic model for the feasibility design (corrective action study preferred option) of the service spillway at El Vado Dam was constructed at Reclamation's Hydraulics Laboratory in Denver, Colorado. Cavitation index value at the worst location was 0.36, which was greater than 0.20 value at which damage typically occurs. The study concluded that such a spillway design does not require extraordinary aeration ramps or other features to promote air entrainment; cavitation potential can be mitigated with the use of appropriate construction tolerances [7]. Nazari et al. (2015)

[8] optimized dimension of the plunge pool and flip buckets of five different spillways using hydraulic model studies. By analyzing the data, relations for dynamic values of maximum and minimum pressures and their location along the flip bucket were extracted. Moreover, their results showed that the entrance and exit sections of the bucket encounter cavitation hazard.

Ozturk and Aydin (2009) [9] used ANSYS-FLUENT model to study aeration in three-dimensional simulation of spillways to prevent cavitation phenomenon. Numerical simulation results were compared with the measurements of the spillway physical model; numerical results were in agreement with the experimental results. Dehdar-behbahani and Parsaie (2016) [10] studied flow pattern in Balaroud Dam spillway's guide wall numerically and showed that the RNG-K-ε is the best model producing the cross waves along the chute spillway. Eskanadari Sabzi and Afrous (2015) [11] investigated the cavitation in 12 models of USACE[1] ogee spillway type at different slopes using ANSYS-FLUENT and k-ε (RNG) turbulence model. They concluded that reduction of the slope of the spillway led to an increase in cavitation index, thus, the likelihood of cavitation occurring plummeted. By performing 30 tests on a physical model with five different values of roughness height, Kamanbedast et al. (2014) [12] found that the coefficient of cavitation decreases as roughness values increase.

Ghodousi and Abedini (2016) [13] have examined the effects of slope reduction, changing the slope and transforming it into two slopes, and the convergence of chute transverse in the Dam using WS77 numerical model. The simulation results implied that cavitation index values would be significantly changed by creating two different slopes in the chute spillway. On the other hand, the chute transverse convergence causes an increase in cavitation index. Teng (2017) [14] used the Volume of Fluid (VOF) model to deviate the spillway discharge

[1] US Army Corps of Engineers

coefficient and showed that the VOF model reproduces reasonably the physical model. Naseri et al. (2018) [15] used large eddy simulation and volume of fluid models to simulate the turbulence and free surface, respectively. Results showed that when moving the place of the hydraulic jump at the first 25% length of the stilling basin, pressure fluctuations were on average 42.6% more at downstream of the chute spillway in comparison with bottom outlet. Chakib (2018) [16] applied VOF model to simulate air-water interaction on the free surface flow of stepped spillway and showed that the $k-\varepsilon$ turbulence standard model is in agreement with the experimental results.

In this study, the cavitation phenomenon in Surk Dam spillway was evaluated using a physical model. Additionally, ANSYS-FLUENT software, which solves the Reynolds-Averaged Navier-Stokes (RANS) equations based on the finite volume method [17], was calibrated using experimental data on the above mentioned spillway physical model. The main aim of this study is to investigate the effect of roughness height on the cavitation number along the chute spillway. Because the reduction of roughness height of the chute bed is one of the most appropriate methods for preventing cavitation, it is essential to evaluate the effect of changing the roughness height on the hydraulic parameters and cavitation number.

Materials and methods

Introducing the studied Dam

In the current study, the spillway of Surk Dam earthen-type clay-core was investigated. Table 1 shows some general characteristics of Surk spillway. The Dam was constructed across the Kiar River near Surk village of Chaharmahal Va Bakhtiari Province, west of Iran, with a height of 39 m and an effective reservoir volume of 25 MCM (million m^3), located at longitude and latitude coordinates of 32°03′26″N and 51°03′00″E and altitude of 2100 m above sea level (See Fig. 1) . The purpose of the Dam is the water supply for downstream agricultural lands and flood control. The Dam has a chute-type ogee spillway in which the slope varies across the chute direction with a distance of 73m from downstream of the spillway crest (See Fig.2). The values for the slope of the chute are 14 degree and 28 degree, respectively, before and after the changes occur. The variations of slope provide conditions for flow separation with a potential for cavitation phenomenon to occur. Therefore, the present research has been carried out as Chaharmahal Va Bakhtiari Regional Water Company's requisition.

Fig 1. Location and view of Surk Dam body and spillway

Table 1. Surk Dam spillway general characteristics

Parameter	Value/description
Spillway chute and crest width (m)	20
Design flood flow rate (m^3/s)	231
Spillway ogee equation	$Y=0.216\ X^{1.748}$ *
Spillway upstream facing slope	1:1
Approach depth at upstream face of the Spillway crest (m)	1

*where X = horizontal distance, Y = vertical distance from coordination axis

Cavitation Index

Cavitation indices can be used to evaluate the potential for cavitation damage in a spillway chute. The cavitation index is defined as follows [18]:

$$\sigma = \frac{P - P_V}{{}^{1}/{}_{2}\rho V^2} \tag{1}$$

Where, σ is the cavitation index, P is the actual fluid pressure on the given point, P_v is the vapor pressure of water, V is average flow velocity and ρ is density of water (kg/m^3). This equation can be rearranged in free-surface overflow spillway by assuming a vertical arc at the bottom as [18]:

$$\sigma = \frac{\frac{P_a}{\gamma} - \frac{P_v}{\gamma} + \frac{P_0}{\gamma} \pm \left({}^{h}/{}_{g} \times \frac{V^2}{R}\right)}{\frac{V^2}{2g}} \tag{2}$$

where, $\frac{P_a}{\gamma}$ is equal to the ambient pressure; $\frac{P_v}{\gamma}$ is the liquid vapor pressure which is equal to 0.32m water at 25 °C; $\frac{P_0}{\gamma}$ is the head equivalent to water pressure measured in different points of the structure; $\frac{V^2}{2g}$ is the velocity head (m) measured at each level; ${}^{\mathrm{h}}/{}_{\mathrm{g}} \times \frac{\mathrm{V}^2}{\mathrm{R}}$ is the arc-induced head difference; h is depth of flow (m); R is the radius of curvature; γ is the unit weight of the fluid (N/m^3) and g is the acceleration due to gravity (m/s^2) . Due to the measured actual pressure in physical mode, $p = \frac{P_0}{\gamma} \pm \left({}^{h}/{}_{g} \times \frac{V^2}{R}\right)$ is no longer needed in the ANSYS-FLUENT software. In contrast, given the arc radius of 5.9 m in spillway crest of physical model, the arc-induced difference in elevation will be equal to $\frac{hv_0^2}{88/57}$, which v_0 is the average velocity at the arc place.

Falvey [18] introduced the ranges of cavitation index values for designing spillway, as illustrated in Table 2.

Table 2. Cavitation indices to be considered in design [18]

Design considerations	Cavitation index
No need for protection against cavitation	**>1.8**
Modified by the removal of irregularities	**0.25-1.8**
Design modification	**0.17-0.25**
Protected by aeration galleries with built steps	**0.12-0.17**
No protection is possible, and needs a redesign	**<0.12**

Physical Model

In addition to the mathematical model, the physical model was used in the current study at Shahrekord University hydraulic laboratory. By preparing hydraulic laboratory facilities and providing basic information, the scale of model was specified so that, firstly, laboratory space became geometrically and dimensionally adequate; secondly, the existing flow capacity will determine the model dimensions. Based on our survey study and due to the fact that gravity is the dominant force in the free overflow, the physical model was designed based on the dynamic similarity with Froude number with a geometry scale of 1:50. Therefore the physical model was made of Plexiglas with the desired geometric features. Front and side views of the physical model are shown in Figs. 3a and 3b. The width of the model was 0.4 m and was installed at the end of the main flume with 0.6 m width and depth and 20 m length. Pumping system and water cycle in the laboratory were capable of supplying up to 70 l/s flow rate inside the flume. To ignore viscosity effects, Reynolds number was controlled to be at least 10^5; additionally, in order to minimize the effect of surface tension and eliminate its adverse effects, Weber number was checked to be always greater than 100 [19].

For measuring the flow rate a triangle weir set at the end of the system with a notch angle of 90 degrees and the following calibrated equation was used;

$$Q = 1.417H^{2.5} \quad (3)$$

Where Q is flow rate (m^3/s) and H is the head on the weir (m).

In order to measure pressure, piezometers were installed along the chute spillway in 26 positions, as shown in Fig. 2 which the numbers to the top of the figure are the numbers of the piezometers row. The piezometer tubes were connected to the piezometer tips which were inserted through holes drilled in the sheet Plexiglas, pasted in place, and finished flush with the surface. The finishing of piezometers in the models was done meticulously to prevent measurement errors that would result from improper installation. Sizes of tubing for connecting piezometers to manometers were selected 2.5 mm inside diameter. For the sake of convenience, piezometers were placed on board; and in order to achieve high accuracy in measuring the height of the water column in piezometers, the board was situated at an angle of 30 degree to the floor in the laboratory [Figs. 3c and 3d].

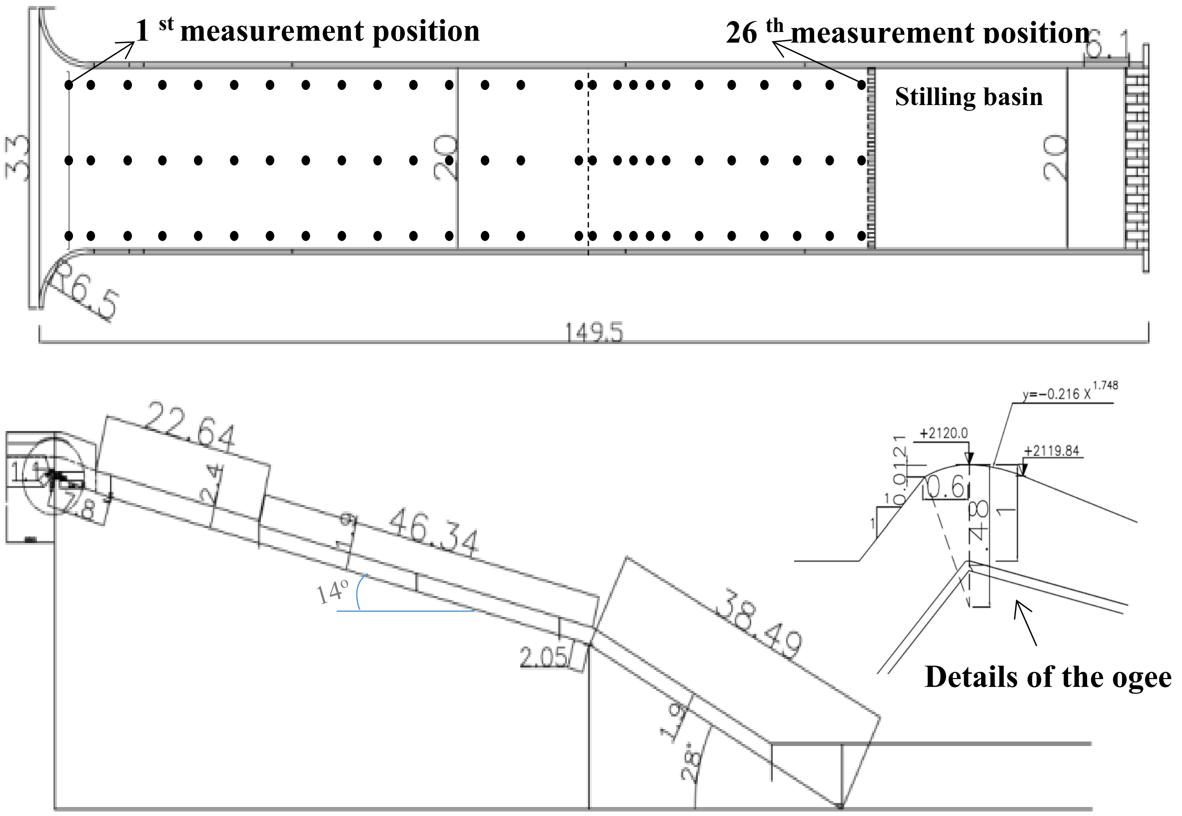

Fig. 2. **The location of flow parameters measurement in Surk Dam spillway.**

Fig. 3. a. front view of the physical model; b. Side view of the physical model; c. view of piezometers installed; d. the picture of the piezometers board

ANSYS-FLUENT software

FLUENT is capable of solving numerically the Navier-Stokes equations of the turbulent flow, which have been widely used in computational fluid dynamics (CFD) applications [17]. This software is one of the most comprehensive computational fluid dynamics software, which benefits from a finite volume approach to convert the governing equations to the algebraic ones. For simulating two-dimensional and three-dimensional hydraulic phenomena, different turbulence models and multiphase problem-solving methods could be taken into account.

ANSYS FLUENT's interactive solver set-up, solution, and post-processing make it easy to pause a calculation, examine results with integrated post-processing, change any setting, and then continue the calculation within a single application. The integration of ANSYS FLUENT into ANSYS Workbench provides users with superior bi-directional connections to all major CAD systems, powerful geometry modification and creation with ANSYS DesignModeler and advanced meshing technologies in ANSYS Meshing. It allows bringing the easy drag-and-drop transfer of data and results to share between applications (e.g. to use a fluid flow solution in the definition of a boundary load of a subsequent structural mechanics simulation). It should be noted that ANSYS FLUENT applies limiting values for pressure, static temperature, and turbulence quantities. The purpose of these limits is to keep the absolute pressure or the static temperature from becoming 0, negative, or excessively large during the calculation, and to keep the turbulence quantities from becoming excessive.

Governing equations

The family of Reynolds-Averaged Navier-Stokes (RANS) models is the most widely used turbulence modeling approach and offers the most economical approach for computing complex turbulent industrial flows. In this approach, the Navier Stokes equations split into mean and fluctuating components. The total velocity u_i is a function of the mean velocity $\bar{u}_i$ and the fluctuating velocity $\acute{u}_i$ as shown in the following equation [17].

$$u_i = \bar{u}_i + \acute{u}_i \tag{4}$$

The continuity and momentum equations incorporating these instantaneous flow variables are given by:

$$\frac{\partial}{\partial x_j}\left(u_i \mathrm{u}_j\right) = -\frac{\partial \mathrm{p}}{\partial x_j} + \frac{\partial \tau_{ij}}{\partial x_j}\rho g_i \tag{5}$$

$$\frac{\partial u_i}{\partial x_j} = 0 \tag{6}$$

$$\tau_{ij} = \left[\rho(v + v_t)\left(\frac{\partial u_i}{\partial x_i} + \frac{\partial u_j}{\partial x_i}\right)\right] - \left[\frac{2}{3}\rho(k + v_t)\frac{\partial u_i}{\partial x_i}\delta_{ij}\right] \tag{7}$$

Where, $u_i$is speed agent in x_i direction, u_j is speed agent in x_j direction, p is total pressure, ρ is fluid density, g is acceleration of gravity, τ_{ij} is stress tensors, $\boldsymbol{v}$ is kinematic viscosity, $\boldsymbol{v}_t$ is turbulence viscosity, k is kinematic energy.

Turbulent models

ANSYS-FLUENT software is capable of solving the Reynolds stress terms using a wide range of turbulent models. The accuracy of solving RANS equations depends on the turbulence model to determine the Reynolds stress terms. The k-ε and k-ω are two such turbulent models, which provide a good compromise between performance and accuracy [20]. K-ε turbulent model is one of the most popular models to simulate turbulent flows, which involves three solutions methods including RNG[2], standard and realizable. Relying on conducted studies, RNG-based k-ε turbulence model is used in the present study [10 and 11]. The RNG-based k-ε turbulence model is derived from the instantaneous Navier-Stokes equations, using a mathematical technique called “renormalization group" (RNG) methods. The analytical derivation results in a model with constants different from those in the standard k- ε model, and additional terms and functions in the transport equations for k and ε, which are illustrated as follows [21]:

$$\frac{\partial}{\partial t}(\rho k) + \frac{\partial}{\partial x_i}(\rho k u_i) = \frac{\partial}{\partial x_j}\left(a_k \mu_{eff} \frac{\partial k}{\partial x_j}\right) + G_k + G_b - \rho\varepsilon - Y_M + S_k \tag{8}$$

$$\frac{\partial}{\partial t}(\rho \varepsilon) + \frac{\partial}{\partial x_i}(\rho \varepsilon u_i) = \frac{\partial}{\partial x_j}\left(a_\varepsilon \mu_{eff} \frac{\partial \varepsilon}{\partial x_j}\right) + C_{1\varepsilon}\frac{\varepsilon}{k}(G_K + G_{3\varepsilon} G_b) - C_{2\varepsilon}\rho\frac{\varepsilon^2}{k} - R_\varepsilon + S_\varepsilon \tag{9}$$

Where, G_k represents the generation of turbulence kinetic energy due to the mean velocity gradients, G_b is the generation of turbulence kinetic energy due to buoyancy, Y_M represents the contribution of the fluctuating dilatation in compressible turbulence to the overall dissipation rate, R_ε is an additional term in the ε equation, the quantities α_k and α_ε are the inverse effective Prandtl numbers for k and ε, respectively, S_k and S_ε are user-defined source terms, $C_{1\varepsilon}$, $C_{2\varepsilon}$ and $C_{3\varepsilon}$ are constants and $\boldsymbol{\mu_{eff}}$ is effective viscosity.

Meshing process and model evaluation

[2] Re-Normalisation Group

Surk Dam spillway model was meshed with Gambit software. Gambit is a software package designed to help analysts and designers build and mesh models for computational fluid dynamics (CFD) and other scientific applications. Gambit receives the user input by means of its graphical user interface (GUI). The Gambit GUI makes the basic steps of the building, meshing, and assigning zone types to a model simple and intuitive, yet it is versatile enough to accommodate a wide range of modeling applications.

In order to reduce the scaling effects in the numerical simulation, the model was designed and implemented in its true dimensions. In order to accomplish the mesh-independent process as a part of the model calibration, the model was run with four meshing numbers including 87412, 75432, 64624 and 44631 triangular cells. Comparing the results of the model with 87412 and 75432 cells showed no significant difference (See Fig.4). For all cases, therefore, the same mesh with 75432 elements was considered in this study.

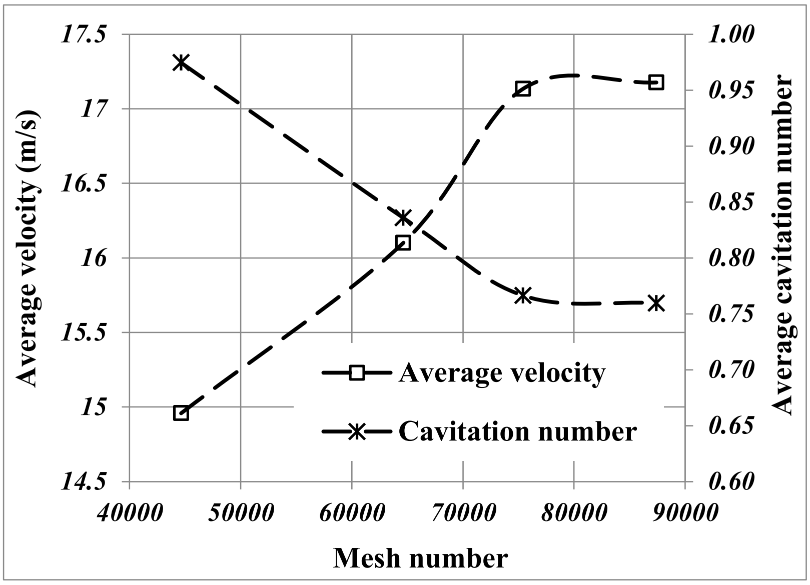

Fig.4. Validation of mesh independency, average velocity and cavitation number versus mesh number

In addition, to obtain a numerical model with the highest level of accuracy, the boundary layer element was applied in the numerical simulation. Boundary conditions were imposed on the numerical model with the numerical models and assumed as the following [Fig.5]:

1. Inlet boundary condition at the inlet, the velocity of flow was considered to set up to the reservoir water level and above that it was considered as a fixed wall
2. Outlet boundary condition, the outflow was set as pressure outlet, to have constant pressure outflow
3. Wall condition, the wall was considered to be at the surface concrete of the chute spillway
4. The top of the domain area was assigned as pressure outlet. Moreover, the initial condition was imposed taking the velocity at the entrance into account.

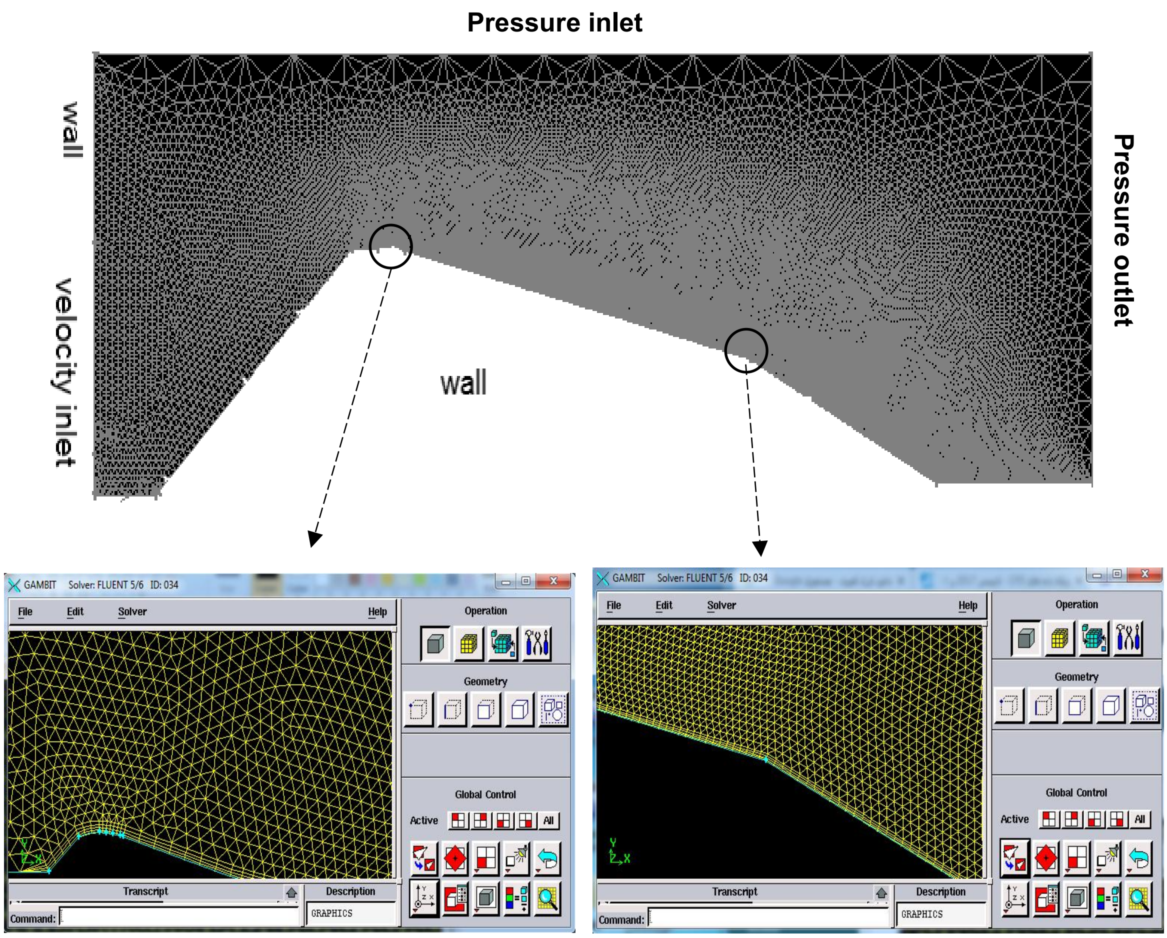

Fig. 5. **Surk Dam spillway boundary conditions and the mesh network**

Two-phase flow solution

Since the cavitation is a two-phase phenomenon consisting of atmosphere and water, VOF model was used for two-phase flow simulation and surface calculations. VOF method is based on the principle that two or more fluids are not combined together. For each phase in the model, one variable is regarded as that phase volume fraction in the computational cell. In each control volume, the total volume fractions for all phases are equal to one. The fluid-volume scheme is assumed to have a point boundary between two phases at which the numerical value of the volume fraction parameter is 0.5 [22]. There are three possibilities of fluid volume fraction (aq) in the cell as,

A.) aq = 0, cell is devoid of fluid.

B) aq = 1, cell is full of fluid.

C) 1> aq> 0, cell owns joint surface between two or more fluids.

In this study, the simulations were performed with five flow rates, as illustrated in table 3, and with respect to the measured values of the flow parameters, such as pressure, velocity, and flow depth, the model was calibrated and validated by changing of the roughness height. The calibrated value of the roughness height was obtained at 2.5 mm. Finally, the cavitation index was calculated at all positions which are shown in Fig. 2. If the numerical results were in a good agreement with the experimental data, the numerical model would be appropriate for our numerical study.

Table 3. Different flow discharge values used in this study

Exp. No.	1*	2	3	4	5
Flow rate in prototype (m^3/s)	234	176.73	151.70	110.80	73.41
Flow rate in physical model (l/s)	13.24	10.00	8.58	6.27	4.15

* Design flow rate

Results and discussion

ANSYS-FLUENT model was calibrated using experimental data from the physical model. After model calibration, the simulation of data was performed for model verification at flow rates lower than the design flow rate, and the results were compared with those achieved from the physical model. Fig. 6 shows a view of the water surface flow through the spillway from the numerical model.

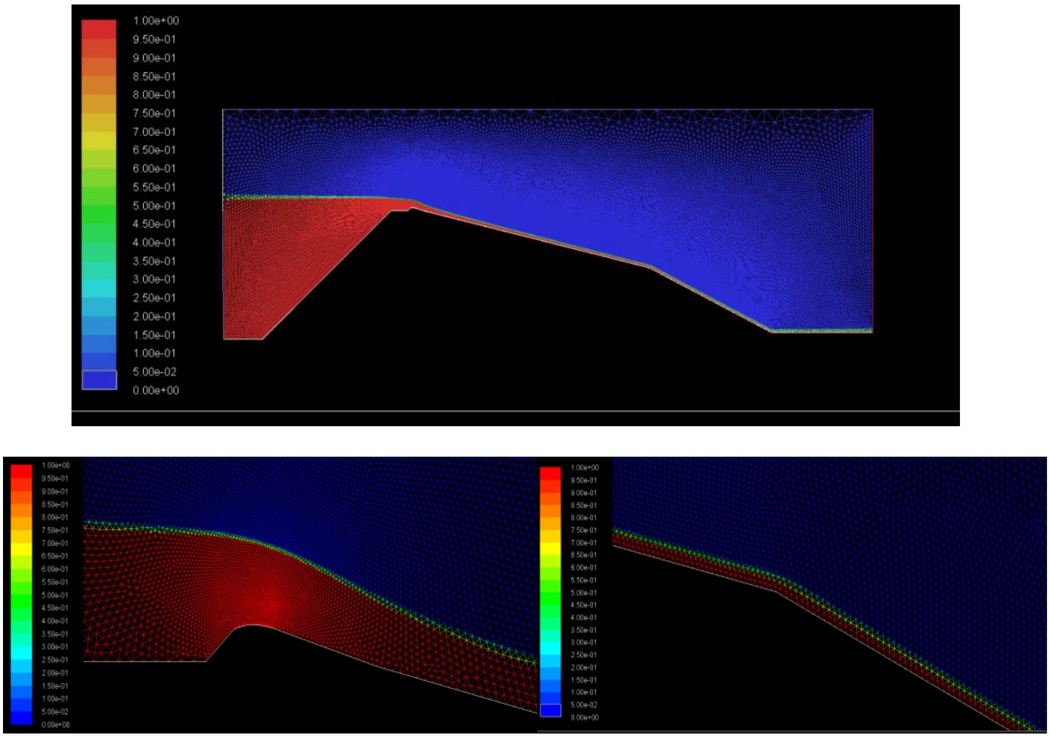

Fig.6. A view of the water surface flow through the spillway from the numerical model.

Results of the simulated model were evaluated by calculating the root-mean-square error (RMSE) and normalized root mean square error (NRMSE). Table 4 represents a comparison of different parameters in ANSYS-FLUENT software and physical model. The statistical parametric equations are defined as:

$$\mathrm{RMSE} = \sqrt{\frac{\Sigma(x_l - x_m)^2}{n-1}} \tag{10}$$

$$NRMSE = \frac{\mathrm{RMSE}}{\bar{x}_l} \times 100 \tag{11}$$

Where, x_m: the values of numerical model, x_l is lab measured values and n is the number of data and $\bar{x}_l$ is the mean value of the lab measurements.

Also the average values of Reynolds number and Froude number obtained from the physical and numerical models for different flow rates and RMSE and NRMSE values of these parameters are illustrated in table 5.

Table 4. RMSE and NRMSE values associated with water depth, velocity, and pressure parameters between experimental and numerical models

Exp. No.	Flow rate (m^3/s)	Depth		Velocity		Pressure	
		RMSE	NRMSE%	RMSE	NRMSE %	RMSE	NRMSE %
1	234	0.058	6.98	0.574	3.38	0.052	5.28
2	176.73	0.057	7.91	0.723	5.117	0.05	5.07
3	151.7	0.062	10.64	0.921	6.66	0.086	8.61
4	110.8	0.056	10.62	0.741	5.623	0.11	11.65
5	73.41	0.043	10.51	0.68	5.89	0.19	19.89

Table 5. Statues of Reynolds number and Froude number obtained from physical and numerical models

Flow rate (m^3/s)		**234**	**176.73**	**151.70**	**110.80**	**73.41**
Reynolds number	Average values (physical model)	12,787,673	9,347,401	7,488,286	6,152,915	4,153,413
	Average value (numerical model)	12,027,173	8,926,200	7,387,561	5,577,645	4,025,209
	RMSE	1,055,240	692,509	510,398	770,613	482,543
	NRMSE (%)	8.3%	7.4%	6.8%	12.5%	11.6%
Froude number	Average values (physical model)	6.54	5.90	6.17	4.19	6.44
	Average value (numerical model)	6.83	6.31	6.75	4.34	6.72
	RMSE	0.42	0.51	0.63	0.23	0.41
	NRMSE (%)	6.5%	8.6%	10.3%	5.5%	6.3%

Cavitation index in physical and numerical models

In order to assess and control the occurrence of cavitation, data such as average velocity and pressure applied on the bottom in different parts of the structure were studied. The necessary data were taken from the two-center axis and the sidewall at different points to calculate the cavitation index. According to equations 1 and 2 and also the values of the parameters obtained from numerical and physical models, the cavitation index was calculated at any section of spillway. In Figs. 7 to 9, the curve of the variations of cavitation index values along the spillway longitudinal axis in numerical and physical models are given for the first, fourth and fifth flow rates. In order to evaluate the accuracy of the numerical model, RMSE, NRMSE and p-value were computed for different flow rates. The results (Table 6) show that there is no significant difference in the cavitation index between experimental and numerical models at 95% confidence interval. That means the accuracy of the numerical model is acceptable at 95% confidence interval [23].

The occurrence of cavitation in this study is determined on the observations proposed by Falvey (1990) illustrated in table 2. As indicated by the cavitation rate curves, the measured cavitation index along the Surk Dam spillway has been continuously decreased. According to the Fig. 7 and table 4, it is obvious that when the designed flow rate passes over the spillway, no cavitation protection is needed for up to 3 m in the downstream of the spillway crest. On the contrary, at a distance of 3 m from the spillway crest, cavitation index reaches 1.8 and from this section, the value of the index decrease due to increasing flow velocity. This trend continues to a distance of 103 m from the crest. Based on Falvey's [18] recommendation, the flow range above the Surk Dam spillway should be modified by correcting irregularities and roughness of the concrete surface and any further decline should be prevented.

The cavitation index was computed and observed to be less than the critical value (σ =0.25) at a flow rate equal to design flow discharge and between 25 and 26 measuring piezometers i.e., at a distance of 103 m from the end of the chute. The lowest cavitation index at 107.3 m from the crest was computed to be 0.249 and 0.237 for the physical model (in the central axis) and numerical model, respectively. The calculated index in this part of the chute ranges from 0.17 to 0.25. According to the Falvey's recommendations [18], modifications should be carried out when a flow rate greater than the designed flow that passes over the spillway to increase the cavitation index in the Surk Dam spillway. Figs. 8 and 9 demonstrate cavitation index variations of the fourth (mean) and fifth (least) flow rates. As shown in the figures, increasing the flow rate reduces cavitation index values so that the index value for the maximum flow rate to be passed from the critical value at the end part of the chute spillway. Additionally, at flow rates lower than the design flow rate, cavitation index in the chute spillway was between 0.25-1.8, which indicates modification requirements by the removal of irregularities of the chute surface concrete are needed. In this regards, the results from both numerical and physical models agree.

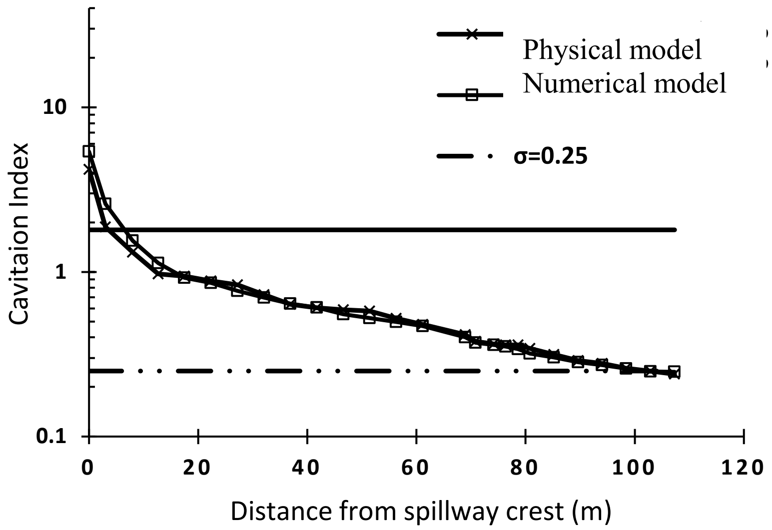

Fig. 7. Variations of cavitation index along the spillway in numerical and physical models at maximum flow rate

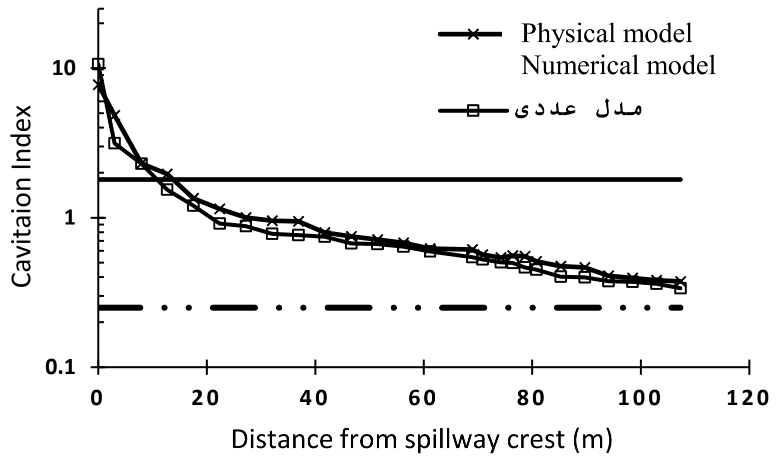

Fig. 8. **Variations of cavitation index along the spillway in numerical and physical models for Q = 110.8 m³/s**

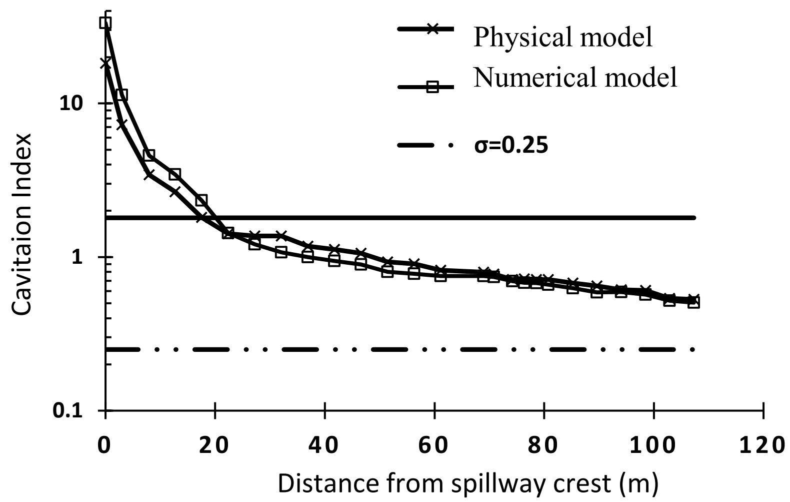

Fig. 9. **Variations of cavitation index along the central axis of the chute spillway for Q = 73.41 m³/s**

Table 6. RMSE, NRMSE and p-values associated with cavitation index parameters between experimental and numerical models

Flow rate (m3/s)	234	176.73	151.7	110.8	73.41
RMSE	0.081	0.106	0.081	0.165	0.331
NRMSE	9.81%	11.55%	8.55%	15.74%	17.75%
P-Value	0.262	0.430	0.225	0.069	0.375

Cavitation index for different roughness heights

In light of the results from the current study and Falvey's [18] recommendations, modification the flow by removing unevenness and reducing roughness height is required. Hence, in order to clarify the influence of modifying the chute surface on the variation of the values of the cavitation index, ANSYS-FLUENT numerical model was calibrated for the roughness in the base case. This will help us to choose an optimal roughness for modifying the spillway surface. In addition to the base roughness height (k_s=2.5 mm), the model was run for values of roughness height between 1 mm and 2 mm under fixed hydraulic circumstances for the designed flow rate in which the cavitation index was less than the critical value, and then cavitation index was calculated.

Fig. 10 illustrates the variations in values of the cavitation index versus distance for different values of roughness height. Fig. 10 shows that the minimum values of the cavitation index are 0.2906, 0.2733, and 0.2471 for the roughness heights 1, 2 and 2.5 mm, respectively. This shows reducing roughness height increases the values of cavitation index, so that the values get away from the critical value stated by Falvey [18]. On the other hand, this decrease maintains the chute of spillway safer against cavitation occurrence compared to the benchmark state. In order to determine the significant level of the effect of the roughness height on the value of the cavitation index, the statistical significance of t-test was done [23]. The results of this analysis, as illustrated in table 7, show that based on the p-value (probability), there is no significant difference of the cavitation index between the cases of roughness heights of 2.5 and 2 mm at 95% confidence interval and the same result has been obtained for the cases of roughness heights of 2.5 and 1 mm. These results show that the method of “modified by the removal of irregularities” (See table 2), which causes the roughness height of the chute spillway to be reduced, would not change significantly the value of the cavitation index.

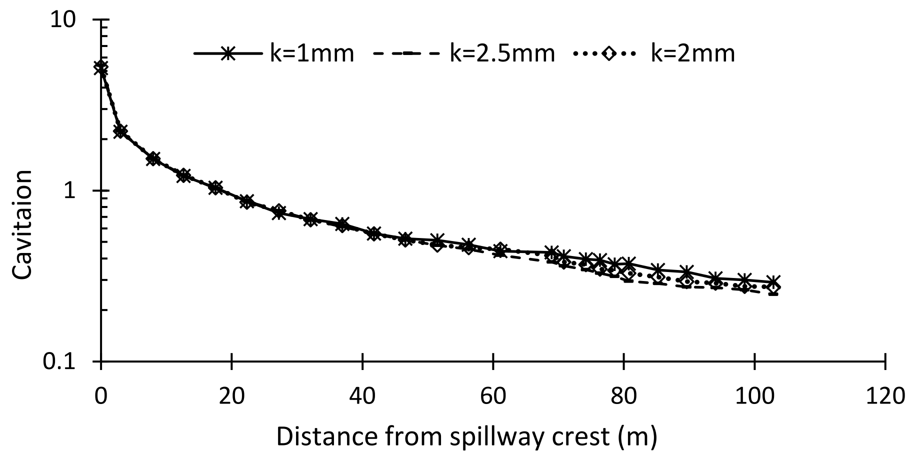

Fig. 10. Variations of cavitation index along spillway for different roughness heights in numerical model for design flow rate

Table 7. The results of statistical significance analysis (t-test)

t-test number	**The first t-test**		**The second t-test**	
variable	Variable 1	Variable 2	Variable 1	Variable 2
Ks (mm)	2.5	2	2.5	1
Mean value of σ	0.812932	0.806234	0.812932	0.824065
Variance	1.080619	1.077335	1.080619	1.035429
Observations	26	26	26	26
Pearson Correlation	0.999969		0.999903	
Hypothesized Mean Difference	0		0	
Degree of freedom	25		25	
t Stat	3.992312		-2.12295	
P-value(T<=t) one-tail	0.000269		0.022134	
t Critical one-tail	1.710882		1.710882	
P--value (T<=t) two-tail	0.000537		0.044267	
t Critical two-tail	2.063899		2.063899	

The results from numerical modeling also show that the reduction on the roughness height decreased the mean velocity. Although reducing the roughness height causes an increase in the flow velocity but any decrease in the roughness height reduces the intensity of flow turbulence. As such, the reduction of flow turbulence causes an increase in the viscosity impact, and flow streamlines will be much more regular compared to the state with higher turbulence. Additionally, the average flow velocity in the boundary layer is reduced [Fig.11].

To verify the abovementioned point of view, the velocity profiles along with flow depth were studied. The results show that reducing the roughness height had an impact on the velocity gradient. Fig. 11 shows velocity variations versus the depth values within a distance of 90 m from the crest. As shown in Fig. 11, reduction of roughness height influenced the velocity gradient, leading to the reduction of the average velocity. This reduction in turn results in an increase in the cavitation index at the chute downstream.

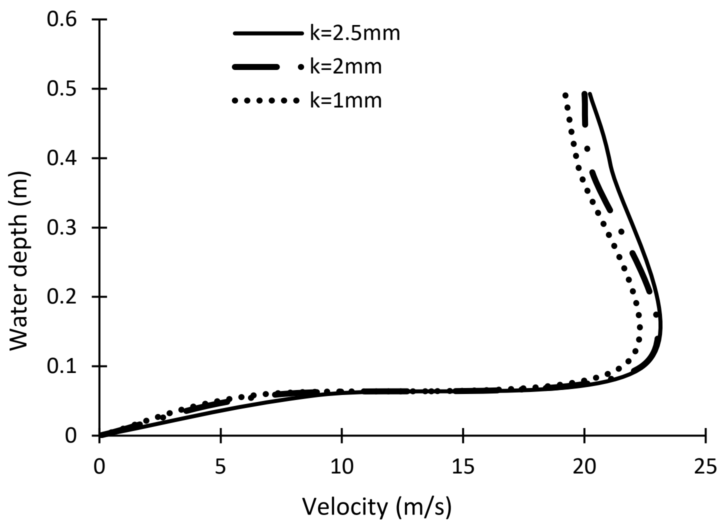

Fig. 11. The variations of velocity distribution by depth for different values of bed roughness heights

Conclusions

Considering the measured and simulated pressure and velocity, results of flows' cavitation coefficient (cavitation index) revealed that the coefficient of cavitation descends over the chute at any flow rate. The minimum value of the cavitation index was calculated to be 0.242 for a flow rate of 234 m^3/s at a point located at a distance of 107.2 m from spillway crest. Considering the calculated cavitation coefficient in the flow rates close to the designed flow rate, the possibility for the reduction of the cavitation index and the occurrence of cavitation exists if the surface roughness and design are not modified. The calculation of cavitation index in flow rates less than design flow rate (the second to fifth flow rates) showed that the modification of flow and irregularities existing on the Surk Dam spillway surface is necessary to prevent the cavitation index reduction. Moreover, the effect of changing roughness on the reduction of the cavitation index for the spillway was numerically simulated in ANSYS-FLUENT software. Results showed that reduction of roughness height influenced the value of cavitation index and the velocity gradient, leading to the reduction of the average velocity. Results showed that the minimum values of cavitation index were 0.2906, 0.2733, and 0.2471 for the roughness heights of 1, 2 and 2.5 mm, respectively. Although these results indicate reducing the roughness height increases the values of the cavitation index, so that the values get away from the critical value stated in previous studies but the statistical significance analysis showed that reducing of the roughness height from 2.5 to 1 mm would not change significantly the value of the cavitation index at 95% confidence interval.

Acknowledgement

Deputy of research in Shahrekord University is highly appreciated because of providing a part of the cost to conduct this research.

References

[1] Bhosekar V. V., V. Jothiprakash and P. B. Deolalikar. Orifice spillway aerator: hydraulic design, Journal of Hydraulic Engineering, 2012, No.6, Vol. 138, pp. 563-572. https://doi.org/10.1061/(ASCE)HY.1943-7900.0000548.

[2] Fiedler, W. Managing Dam Safety Risks Related to Hydraulic of the accuracy es. In B. Crookston & B. Tullis (Eds.), Hydraulic Structures and Water System Management. 6th IAHR International Symposium on Hydraulic Structures, Portland, OR, 2016. pp.508-518. doi:10.15142/T3720628160853.

[3] Lee, W. and J. A. Hoopes. Prediction of cavitation damage for spillways, Journal of Hydraulic Engineering, 1996, No.9, Vol. 122, pp.481–488. https://doi.org/ 10.1061/(ASCE) 0733-9429(1996)122:9(481)

[4] Inozemtsev Y P. Cavitation destruction of concrete and protective facings under natural conditions, Power Technology and Engineering, 1969, No.1, Vol.3, pp. 24-29.

[5] Kells J.A., C. D. Smith. Reduction of cavitation on spillways by induced air entrainment, Canadian Journal of Civil Engineering, 1991, No.3, Vol. 18, pp.358-377. https://doi.org/10.1139/l91-047.

[6] Rajasekhar P., Santhosh. Y V G. and Soma Sekhar S. Physical and numerical model studies on cavitation phenomenon- A study on Nagarjuna Sagar spillway, International Journal of Recent Development in Engineering and Technology, 2014, No.1, Vol.2, pp. 2347-6435.

[7] Heiner B.J., Ch.C. Shupe. El Vado Dam – Service spillway modification - physical model study, Hydraulic Laboratory Techniques, U.S. Department of the Interior, 2017, Report No. HL-2017-02.

[8] Nazari, O., E. Jabbari and H. Sarkardeh. Dynamic pressure analysis at chute flip buckets of five dam model studies, International Journal of Civil Engineering, Transaction A: Civil Engineering, 2015, No. 1, Vol. 13, 45-54.

[9] Ozturk M. and Aydin M. C. Verification of a 3-D numerical model for spillway aerator, Mathematical and Computational Applications, 2009, No.1, Vol.14, pp.21-30.

[10] Dehdar-behbahani, S. and A. Parsaie. Numerical modeling of flow pattern in dam spillway’s guide wall. Case study: Balaroud dam, Iran. Alexandria Engineering Journal, 2016, No.1, Vol. 55, pp. 467–473. https://doi.org/10.1016/j.aej.2016.01.006.

[11] Eskanadari Sabzi, A. and A. Afrous. Examining the effect of cavitation on crest spillway using Ansys-fluent software, Journal of Scientific Research and Development, 2015, No.5, Vol. 2: 303-308.

[12] Kamanbedast AA., M. Bahmani, R. Aghamajidi, The Effect Of Surface Roughness On Discharge Coefficient And Cavitations Of Ogee Spillways Using Physical Models, Journal Of Applied Science And Agriculture, 2014, No.6, Vol.9, pp. 2442-2448.

[13] Ghodousi H. , Abedini A M. Simultaneous effect of convergence and reducing slope of chute construction on the economic of the plan and cavitation Index (Case study: Daharan Dam), Open Journal of Geology, 2016, No.7, Vol.6, pp.617-625. DOI: 10.4236/ojg.2016.67048.

[14] Teng, P.H. CFD modelling of two-phase flows at spillway aerator, TRITA-HYD, 2017, No.02, p 56.

[15] Naseri, F., Sarkardeh, H. and Jabbari, E. Effect of inlet flow condition on hydrodynamic parameters of stilling basins, Acta Mechanica, 2018, No.3, Vol. 229, pp.1415–1428.) https://doi.org/10.1007/s00707-017-2069-z.

[16] Chakib , B. Numerical Study of Turbulent Flow for Moderate-Slope Stepped Spillways, Malaysian Journal of Civil Engineering, 2018, No.1, Vol. 30, pp.57-68.

[17] ANSYS FLUENT 15.0 Theory Guide; 2013.

[18] Falvey H. Cavitation in chute and spillway. Bureau of Recamation. Denever Co.Use, 1990, 145p.

[19] Boes R. and Hager W. H. Two-phase characteristics of stepped spillways, Journal of Hydraulic Engineering, 2003, No.9, Vol. 129, pp.661–670. DOI:10.1061/ (ASCE) 0733-9429.

[20] Aftab S.M.A., Mohd Rafie A.S., Razak N.A., Ahmad K.A.Turbulence model selection for low Reynolds number flows. PLOS ONE, 2016; No. 4, Vol. 11, e0153755.https://doi.org/10.1371/journal. pone.0153755.

[21] Chaudhury D. Introduction to the renormalization group method and turbulence modeling. Fluent Inc. Technical Memorandum TM-107, 1993.

[22] Dargahi B. Experimental study and 3D numerical simulations for a free over flow spillway. Journal of Hydraulic Engineering, 2004, No. 9, Vol. 132, pp.899-907.

[23] Colquhoun D. The reproducibility of research and the misinterpretation of p-values. Royal Society Open Science, 2017, No. 12, Vol. 4:171085. doi:10.1098/rsos.171085.